Ground roll interpolation and attenuation

Ji Li, Daniel Trad

ABSTRACT

Ground-roll attenuation is an essential step in land seismic data processing. Simple methods like bandpass filter or f-k filter can remove the ground roll based on the difference in the frequency domain. However, the performance is often limited due to the spatial aliasing of the ground roll, which causes the overlap of the ground roll with reflections in the frequency domain. An interpolation step of the seismic data can improve the final ground roll attenuation performance. We adopt a convolutional neural network-based framework named Residual dense networks (RDN) to interpolate the seismic data with a strong ground roll and weak reflections. The purpose is to interpolate the strong ground roll and weak reflections simultaneously. We first create a training dataset via the finite different method to train the model. Then we test seismic data interpolation on another dataset, which is not a part of the training dataset. We compare the interpolated shot gather with and without the ground roll. The interpolated results prove that the proposed approach can interpolate the strong ground roll and keep the weak reflections simultaneously. Ather the interpolation, a simple f-k filter is applied to both the synthetic and real data examples to attenuate the ground roll. The result is also compared with the traditional F-X interpolation approach.

INTRODUCTION

Ground-roll attenuation is a significant problem encountered in land seismic data processing. Ground roll can be characterized as low frequency, low velocity and high amplitude coherent noise. It can dominate near-source traces on seismic records and mask weak reflections we are interested in. Ground roll can be effectively attenuated during the acquisition stage using stack arrays (Morse and Hildebrandt, 1989). However, a significant amount of ground roll will remain on the seismic records and must be attenuated using signal-processing approaches.

Numerous methods have been developed over the years to attenuate ground roll noise. The most straightforward approach for ground roll attenuation is using a bandpass filter, which separates the ground roll and primary reflections based on their frequency. For example, Saatcilar and Canitez (1988) use 1D linear frequency-modulated match filters to separate the ground roll from reflections. An F-K filter is another simple way to attenuate the ground roll (Treitel et al., 1967; Beresford-Smith and Rango, 1989). Other ground-roll attenuation approaches include filtering with different transforms, like S-transform (Askari and Siahkoohi, 2008), wavelet transform (Deighan and Watts, 1997; Wang et al., 2012) and radial trace transform (Henley, 2003). Other filterings like SVD filtering (Porsani et al., 2010) and matching filtering (Jiao et al., 2015) can also apply to remove the ground roll. Machine learning-based methods have recently been adopted to solve the ground roll attenuation problem. Yuan et al. (2020) use generative adversarial networks (GANs) to remove the ground roll from the shot gathers. Li et al. (2018) adopted a denoising CNN architecture to treat ground roll attenuation as the denoising problem. The latest development is from (Pham and Li, 2022), combining unsupervised and supervised deep-

learning approaches with three components to remove the ground roll.

Most simple conventional ground roll attenuation methods use filters in the frequency domain. These methods' performance is limited by spatial aliasing in the frequency domain. Therefore, the seismic data must be interpolated before the ground roll attenuation to improve the performance. There are many conventional interpolation methods, such as sparse transform-based methods (Trad et al., 2002; Liu and Sacchi, 2004; Abma and Kabir, 2006; Trad, 2009), rank-reduction-based methods (Trickett et al., 2010; Gao et al., 2013; Jia et al., 2016) and frequency space (f-x) prediction filter-based methods (Spitz, 1991; Naghizadeh and Sacchi, 2007). However, most approaches mentioned above are only suitable for irregularly sampled seismic data obtained using a random acquisition scheme (Gao et al., 2015). For the regularly under-sampled seismic data, spatial aliasing becomes an issue which is the same as the ground roll attenuation problem. An antialiasing strategy must be addressed for regularly sampled seismic data with spatial aliasing in the frequency domain to improve the interpolation performance. The performance of these antialiasing interpolation methods is always sensitive to the parameters used. Recently, with the development of machine learning, many interpolation methods based on the deep learning architecture are proposed like (Wang et al., 2019; Kaur et al., 2019; Wang et al., 2020; Fang et al., 2021). These methods can not only deal with seismic data with spatial aliasing but also don't require the pre-request assumptions like the sparsity and linearity of the seismic data.

This paper will use a convolutional neural network (CNN) based architecture called Residual dense Network (RDN) to interpolate spatial aliased seismic data. A detailed explanation of the network and the design of the training are provided in the theory part. A set of data generated by the finite different method is used for training. After training, a different set is used to test the interpolation performance. Then we use the trained model to interpolate synthetic and real data examples with low-frequency intense ground roll noise. After the interpolation removes the spatial aliasing in the frequency domain, a simple f-k filter is applied to remove the ground roll noise in these datasets.

THEORY

Residul dense Network

The Residual dense network (RDN) was initially proposed by Zhang et al. (2018) for image super-resolution. RDN is a deep neural network architecture that uses dense connections and residual learning to improve the performance of image restoration tasks. It consists of several dense blocks (residual dense blocks), each containing multiple convolutional layers with direct connections between them. The dense connections enable the reuse of features learned in earlier layers, which helps to reduce the vanishing gradient problem and improve the network's performance. The residual connections allow the network to know the difference between the input and output, which helps preserve the image's details.

Zhang et al. (2019) applied it to the seismic data interpolation problem. The architecture of the RDNnet for the seismic interpolation is presented in figure 1. As we can see, the

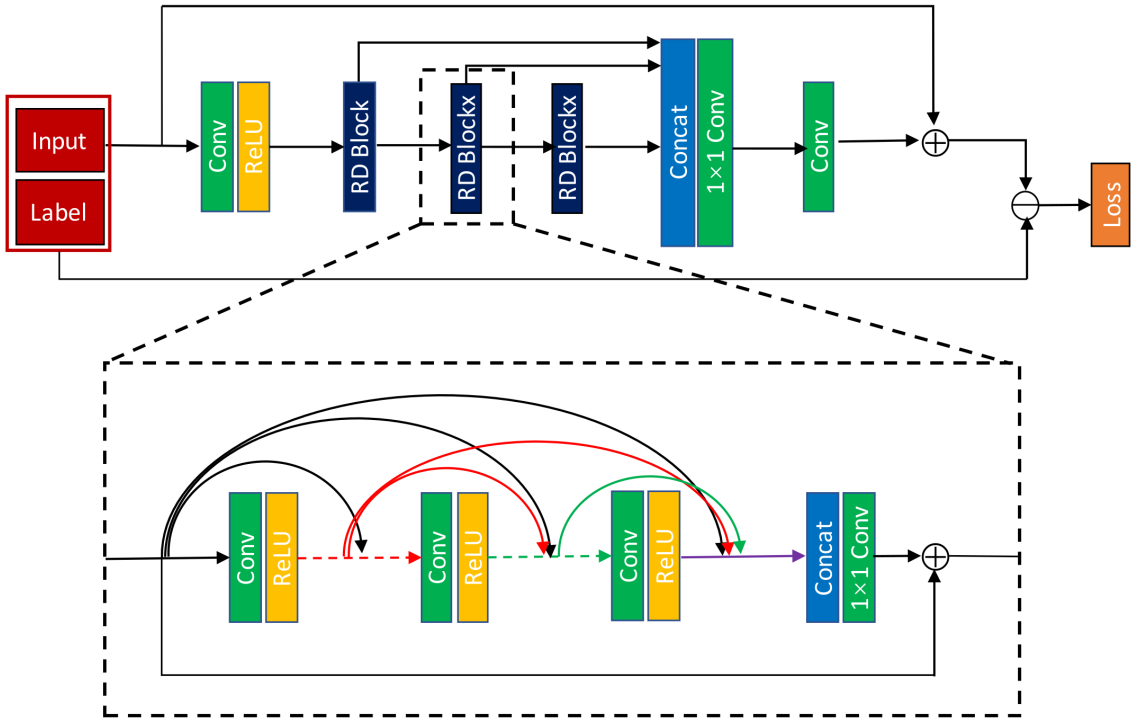

FIG. 1. The architecture of the RDN (From Zhang 2019)

architecture contains three residual dense blocks. Inside each block are three convolutional layers, all connected to each other. As shown in the figure, the outputs of one residual dense block and each layer within the current block can also connect directly to all the subsequent layers through the contiguous memory (CM) mechanism. To apply this architecture to the seismic data interpolation problem, the input will be the decimated seismic data patches. The label will be the original complete seismic data patches. And the output will be the interpolated seismic shot gather patches. We need to sort the interpolated patches back to the shot gathers to get the final interpolated result.

Training data and parameters

Using the Rdnet to interpolate the seismic data with strong ground roll, we first need to generate the training data and training labels. We use the finite different method to create a training dataset. The dataset includes some strong ground-roll and weak reflections. The maximum amplitude of the ground roll is about 100 times the maximum amplitude of the reflections. The dataset consists of seven shot gathers, each containing 1436 receivers and 719 samples on the time axis. We use this dataset as our training labels. We then kill half of the traces regularly, our training input.

We use a package called TensorFlow (Abadi et al., 2016) for the training. We train our model on the small patches instead of the whole shot gather. The input and the labels are divided into overlapped patches with a window size of 32. Figure 2 shows an example of four consecutive input patches and their corresponding labels. After the training, we sort the predicted data patches back into common shot gathers.

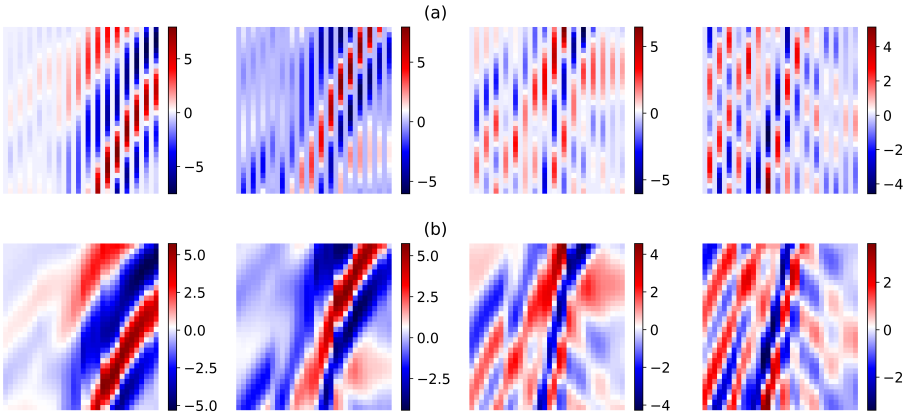

FIG. 2. Four consecutive patches. (a) Decimated patches. (b) Corresponding labels.

We remove all zero patches to save costs before putting the divided patches into the network. We use mean square error (MSE) between the interpolated and labelled data as the loss function. The evaluation metric is defined as the reconstructed data's signal-to-noise ratio, $SNR = 10\log\frac{\|\mathbf{d}_l\|_2^2}{\|\mathbf{d_l}-\mathbf{d_i}\|}$. $\mathbf{d}_l$ is the label and $\mathbf{d_i}$ is the interpolated result. We use the Adaptive momentum algorithm (Adam) (Kingma and Ba, 2014) for the optimizer. We used a variety learning rate initially set at 1e-4, which will decrease after each epoch. The training process will stop when there is no improvement in the signal-to-noise ratio after ten consecutive epochs. The maximum epoch we used is 20. We use the mini-batch to update the parameters and set the batch size to 8. The model with the maximum signal-to-noise ratio will be saved at the end.

EXAMPLES

Seismic data interpolation

Training dataset

First, we test the trained model on the training dataset and compare the interpolated result with the original labels. One training shot gather and corresponding decimated shot gathers are presented in figure 3. The interpolated results and the errors compared with the original labels are shown in figure 4. The interpolated results show some errors, most from the strong ground roll. The main focus of our test is to check whether the weak reflections can be interpolated successfully despite the strong ground roll because we will remove the ground roll at the end.

We compare the interpolated reflections and present the results in figure 5. The amplitude of the reflections in figure 5 is clipped to show the weak reflections better. Figure 5 (a) is the accurate reflections, and part (b) is the interpolated reflections. Most errors come from the ground roll, and the weak reflections are interpolated successfully.

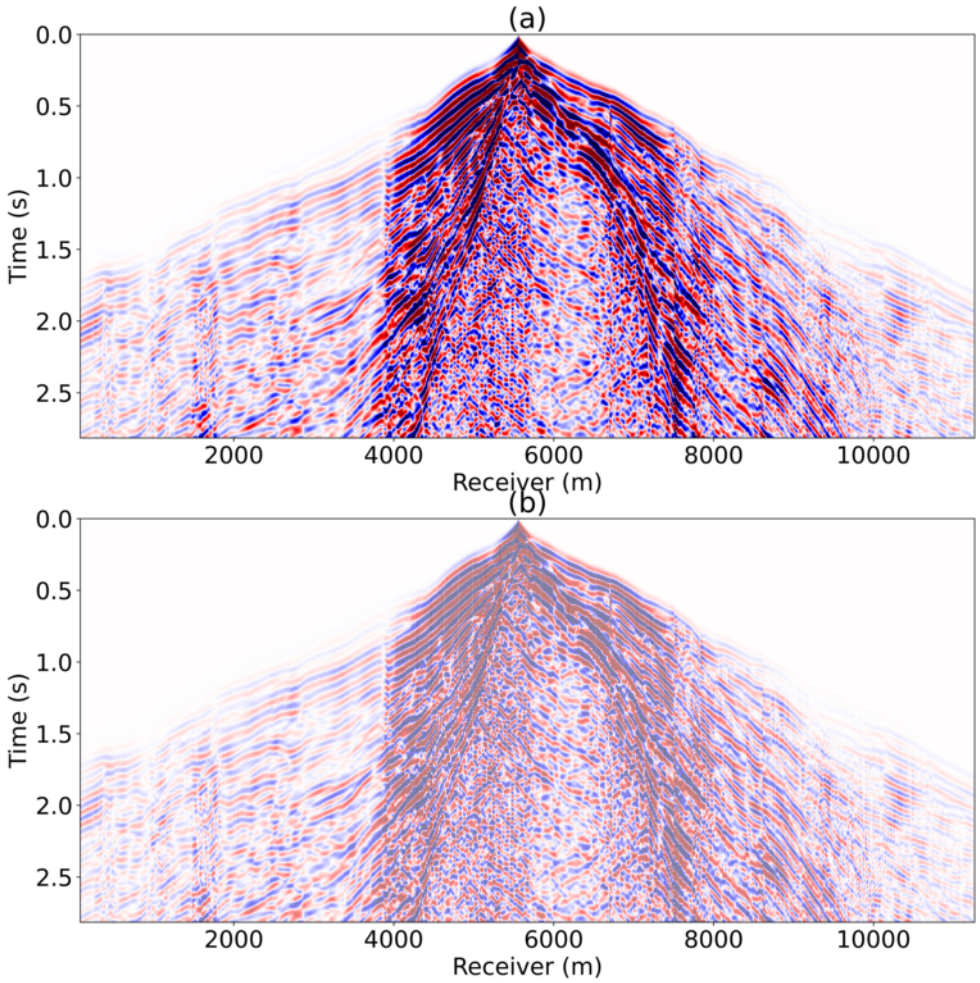

FIG. 3. One of the training shot gathers. (a) Original shot gather. (b) Decimated shot gather.

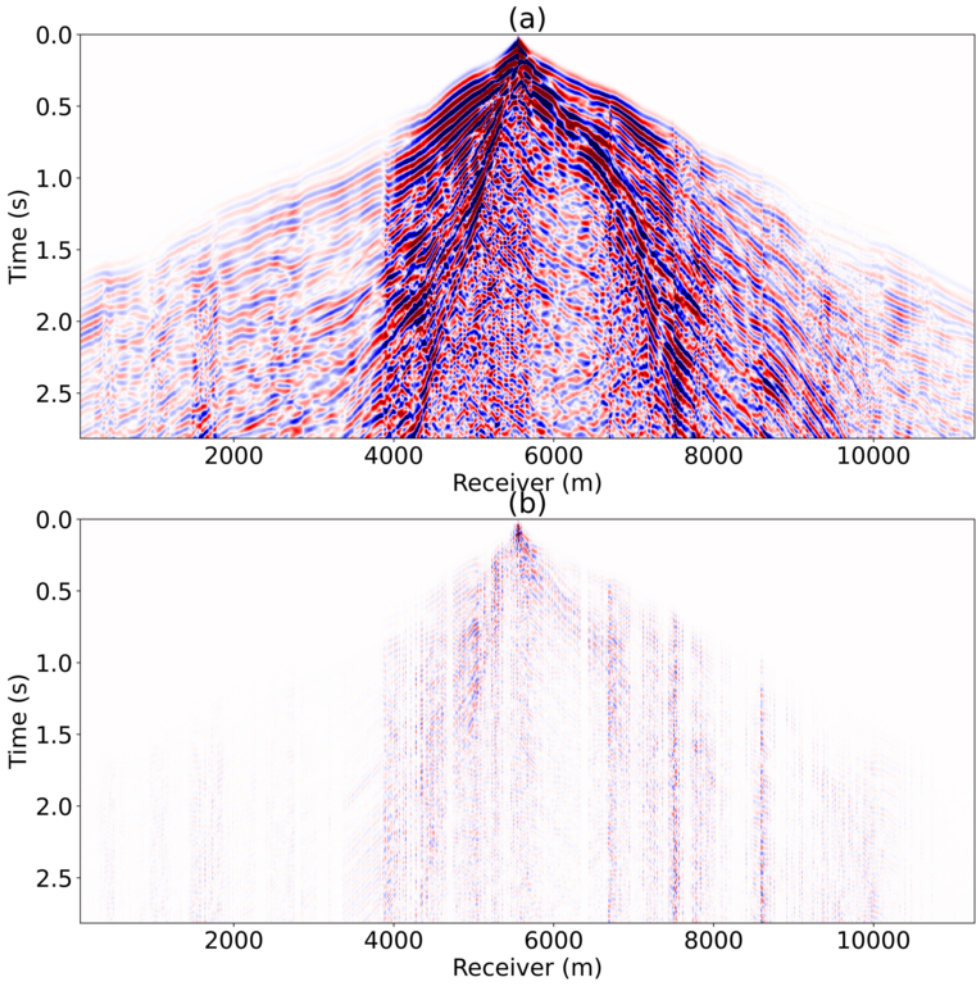

FIG. 4. Interpolated result of one training shot gather. (a) Interpolated shot gather. (b) Errors between interpolated shot gather, and original shot gather.

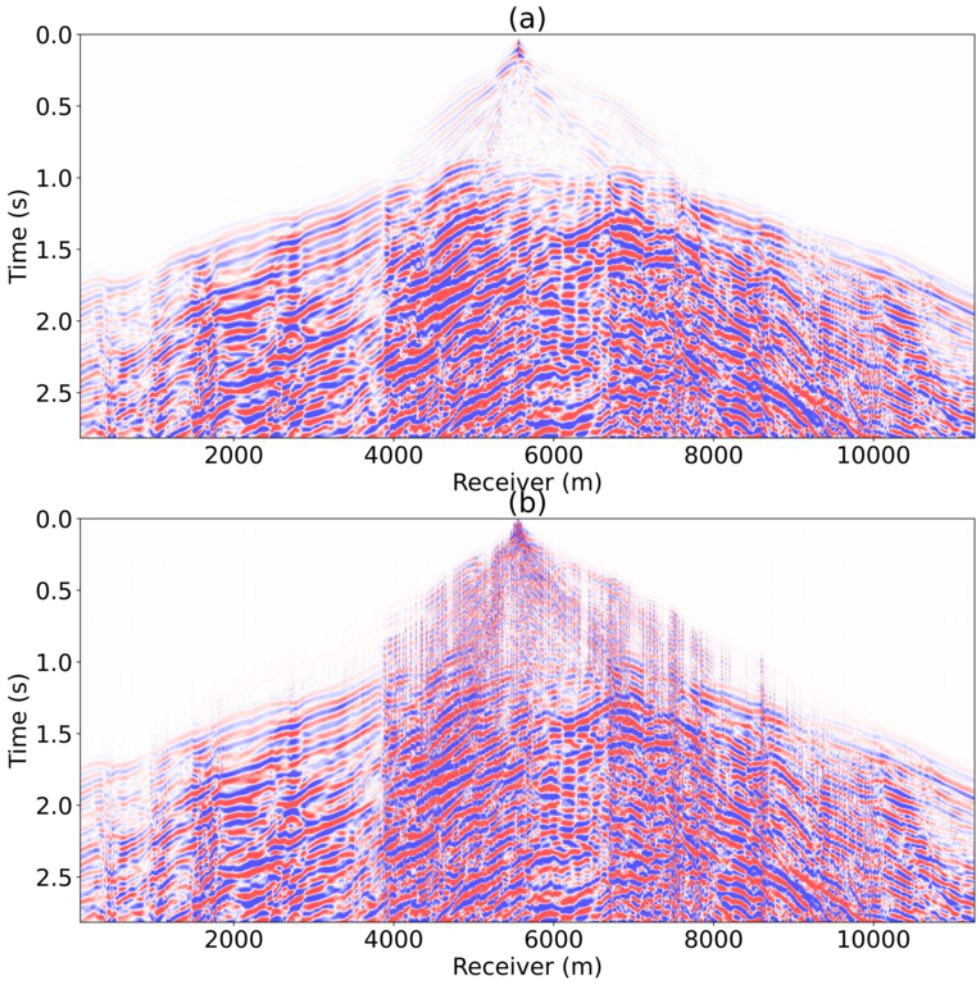

FIG. 5. (a) Original reflections. (b) Interpolated reflections.

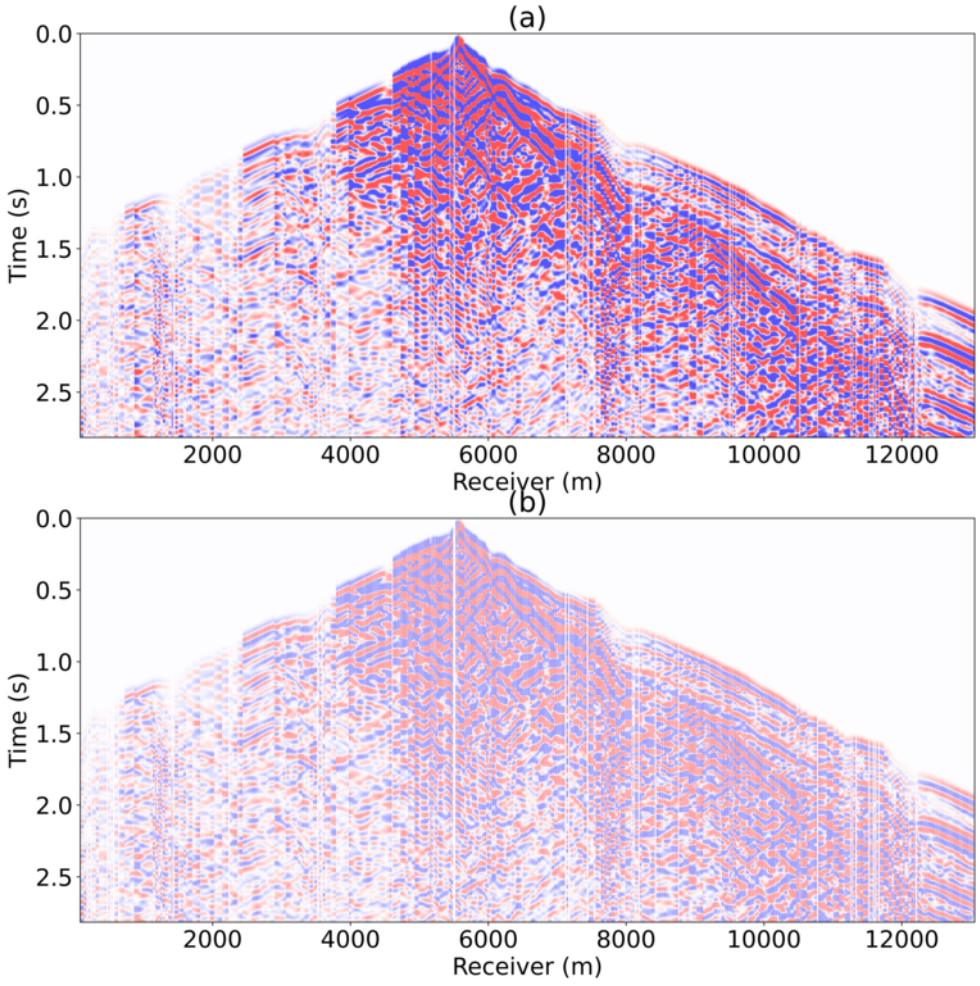

FIG. 6. One of the test shot gathers. (a) Original shot gather. (b) Decimated shot gather.

Test dataset

We then test our trained model with a test dataset not included in the original training dataset. All the figures for this example are clipped to show the weak reflections better. The clipping only applied to the plot. We use the original actual amplitude for the testing. Figure 6 presents a single shot gather from the test data set. The interpolated result is shown in figure 7. Same as the training example, we compare the actual and interpolated reflections in figure 8. Like the training dataset, most errors came from the near-surface ground roll parts, and almost all weak reflections were interpolated successfully. This example proves the method works as it can successfully interpolate a different dataset without putting it in the training process.

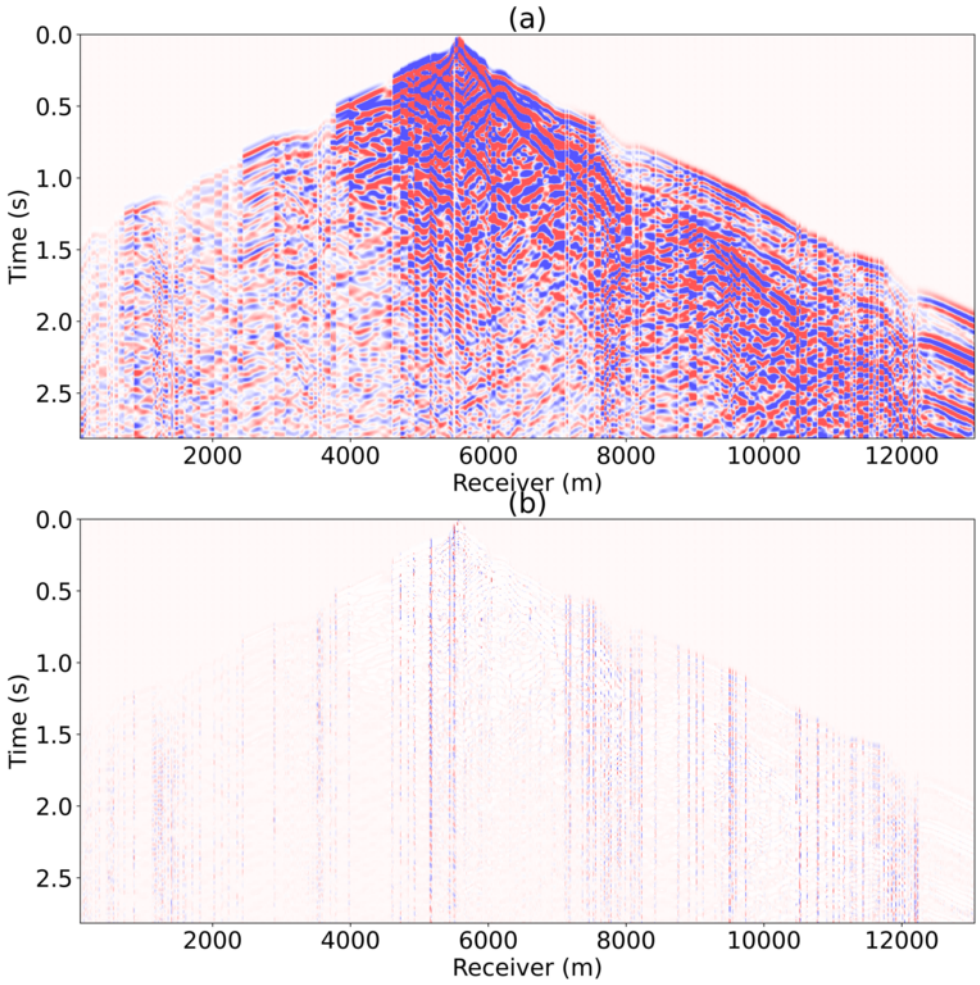

FIG. 7. Interpolated result of one test shot gather. (a) Interpolated shot gather. (b) Errors between interpolated shot gather, and original shot gather.

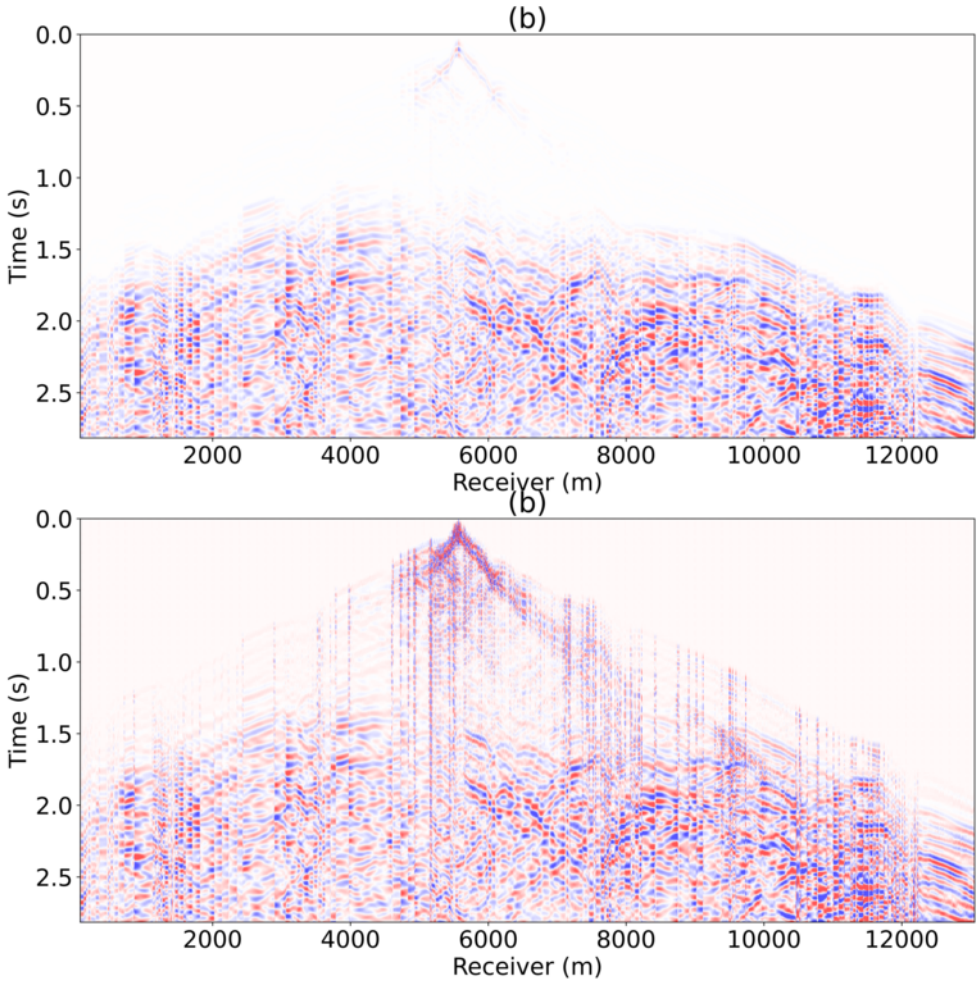

FIG. 8. (a) Original true reflections. (b) Interpolated reflections.

Ground roll attenuation

Synthetic data

Previous examples show that the RDN can interpolate seismic data with the strong ground roll and keep the weak reflection signals simultaneously. After the interpolation, we can apply an F-K filter to remove the ground roll of the interpolated shot gather. In this example, we also compare the performance with a famous conventional interpolation method. Spitz (1991) proposed an F-X interpolation to interpolate the multichannel seismic data. The reason for selecting this method is because that this method can interpolate regularly sampled data. Figure 9 (a) shows a shot gather from the third dataset with intense ground roll noise. The ground roll in this dataset is modified for the test and limited within the low-frequency range. A complex ground roll in the previous example is unsuitable for testing because most conventional methods can not remove them successfully. Figure 9 (b) is the interpolated result by the F-X method, and figure 9 (c) is the result by the previously trained model. We present the corresponding F-K panels of the shot gathers in figure 10. Part (a) indicates strong aliasing noise in the F-K panel of the decimated data. The F-K panel in part(b) shows some repeated noise, indicating that the amplitude of the interpolated trace is weaker than the actual amplitude. And all the aliasing noise disappeared in part (c).

The F-K panel shows that most ground rolls are within the frequency range of 0 to 8 Hz and wavenumber between -0.02 to 0.02 m^{-1}. A simple F-K filter is designed to remove ground roll within this range. Figure 11 presents the result after the ground roll attenuation. Part (a) is the accurate reflections, and part (b) is the shot gather after passing the f-k filter. Compared with the accurate reflections, almost all ground rolls are removed with some reflection distortion.

Real data

We ultimately applied the same process to remove the ground roll in real data examples. Figure 12 presents a real land seismic shot gather. We show the corresponding F-K panels in figure 13. For this real data example, FX and machine learning methods do not work well since the feature is not close to the training dataset. The ground roll part is not interpolated successfully. The F-X panel shows that the FX method can not interpolate ground roll and reflections. And the RDN interpolated the reflection part successfully. The F-X panel also indicates that the ground roll is located around the frequency range between 0 to 17.5 Hz. We attenuated the ground roll of the interpolated result from RDN and presented the result in figure 14.

Figure 15 and 16 present another real data example. The original dataset is already undersampled with spatial aliasing for this shot gather. Therefore we applied the interpolation methods to it directly without decimating it. Again, the RDN method has a better result than the F-X method. We then used a bandpass filter to remove the ground roll. The final result is presented in figure 17.

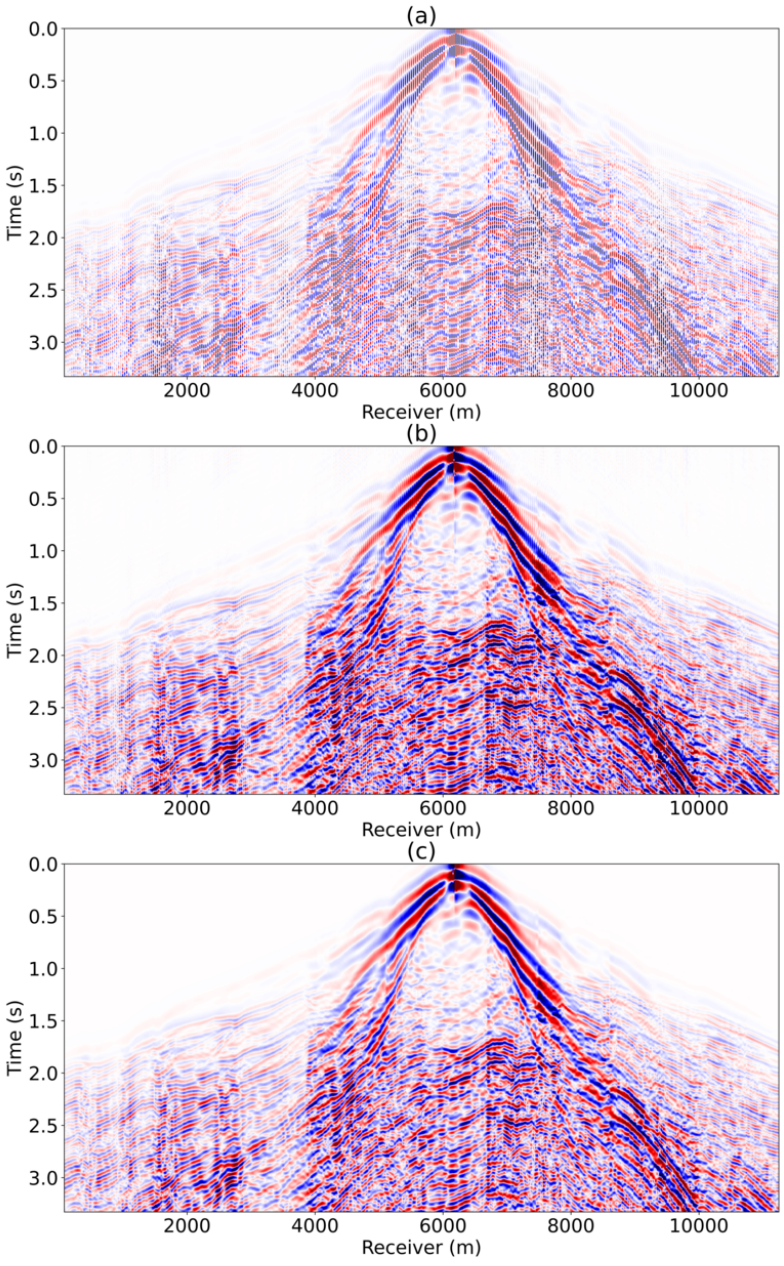

FIG. 9. Shot gather used for ground attenuation test. (a) Decimated shot gather. (b) Interpolated result via FX interpolation. (c) Interpolated result via RDN

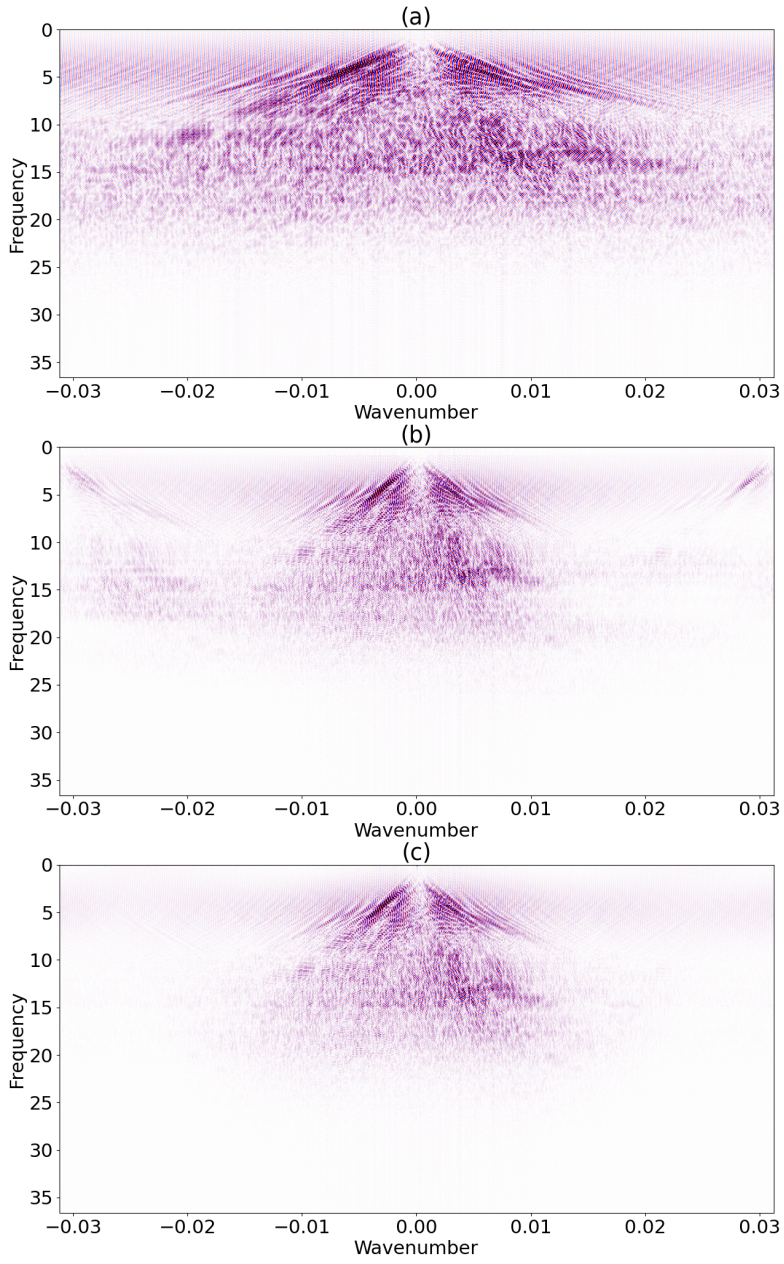

FIG. 10. F-k panel of the test shot gather. (a) F-K panel of the decimated shot gather. (b) F-K panel of the interpolated shot gather via FX interpolation. (c) F-K panel of the interpolated shot gather via RDN.

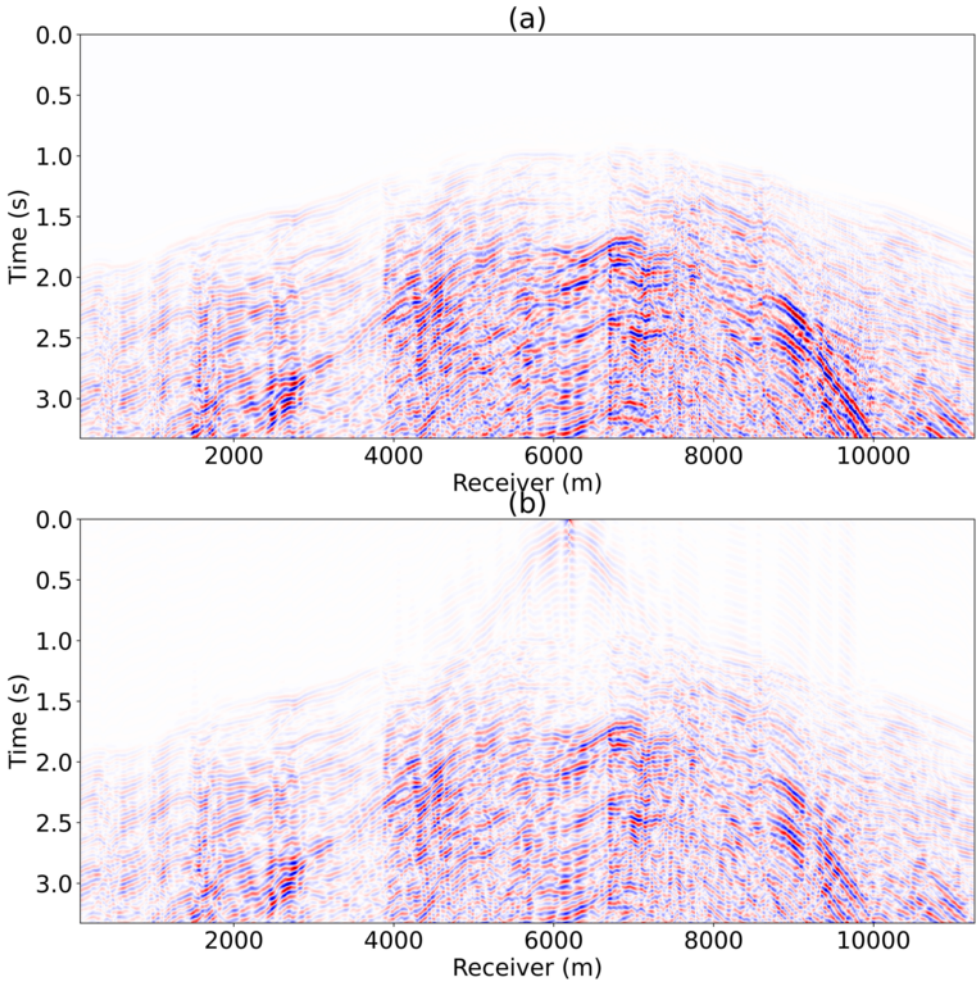

FIG. 11. (a) Original true reflections. (b) Reflections of the interpolated shot gather after applying an F-K filter.

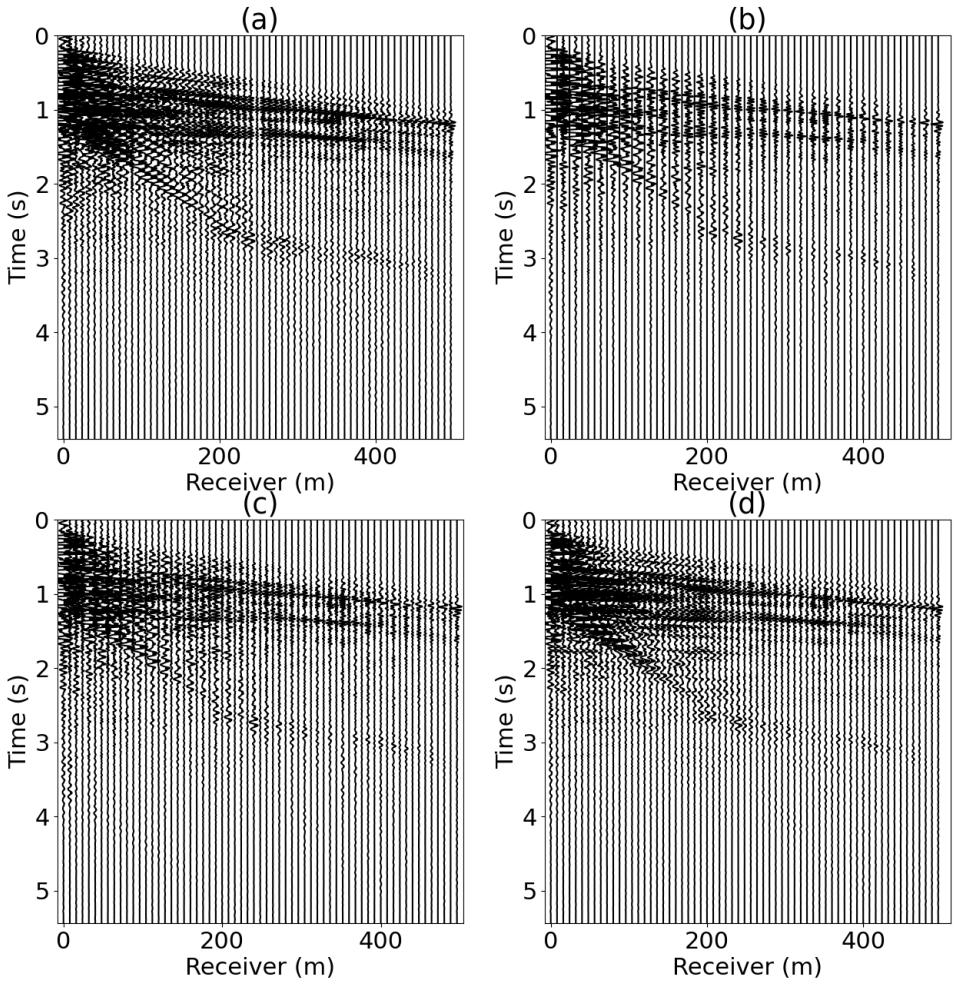

FIG. 12. Real data test. (a) Original shot gather. (b) Decimated shot gather. (c) Interpolated shot gather via FX interpolation. (d) Interpolated shot gather via RDN.

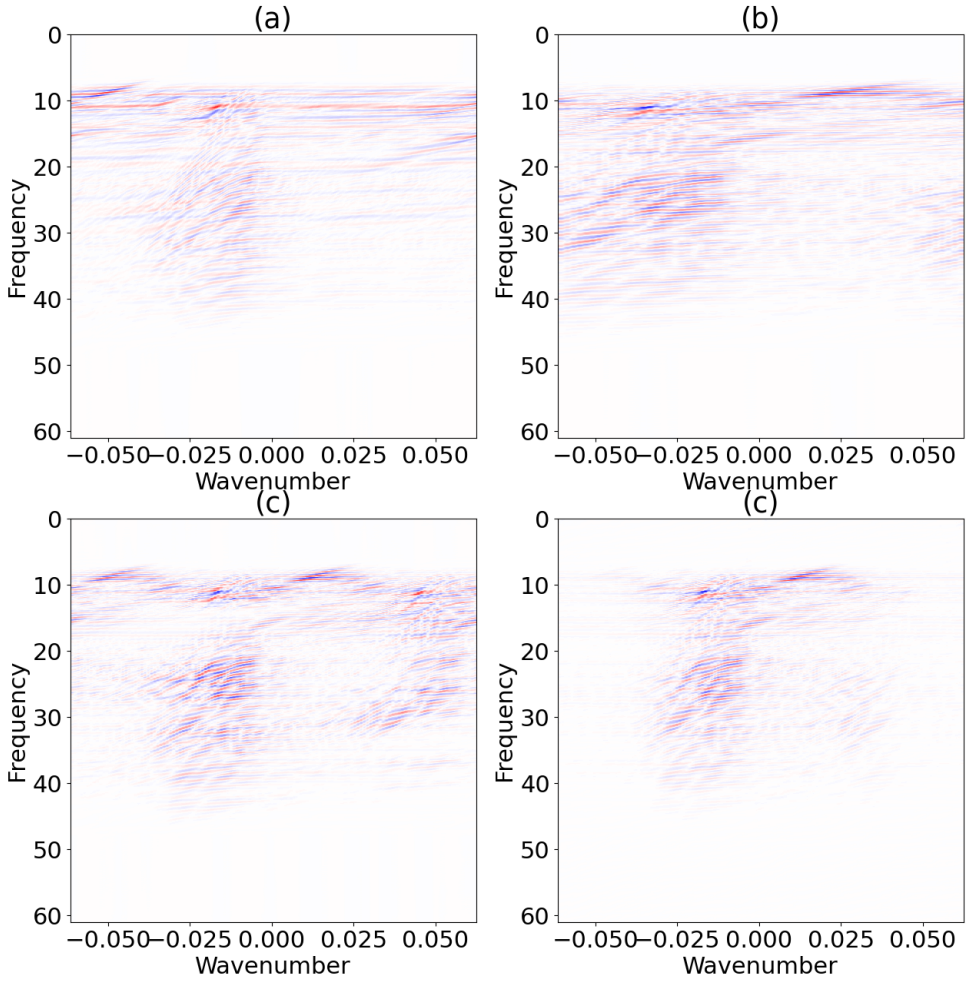

FIG. 13. F-k panel of the real shot gather. (a) F-K panel of the Original shot gather. (b) F-K panel of the decimated shot gather. (c) F-K panel of the interpolated shot gather via FX interpolation. (c) F-K panel of the interpolated shot gather via RDN.

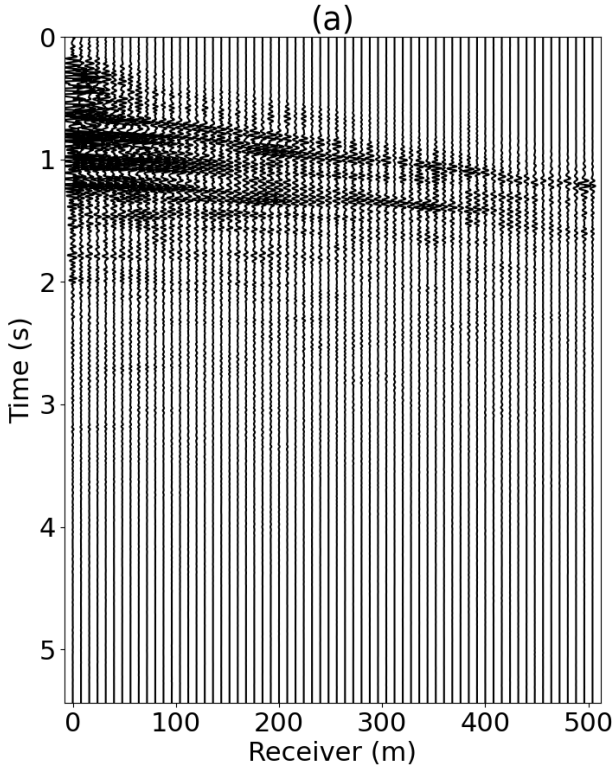

FIG. 14. Final shot gather after interpolation and ground roll attenuation

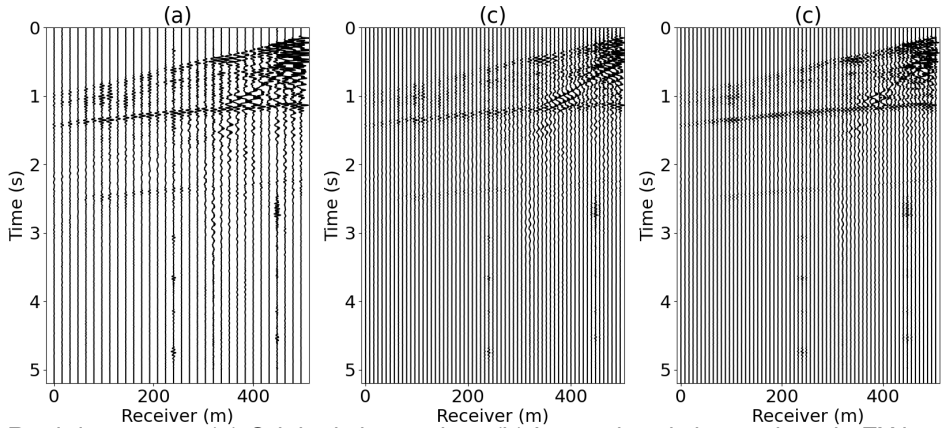

FIG. 15. Real data test 2. (a) Original shot gather. (b) Interpolated shot gather via FX interpolation. (c) Interpolated shot gather via RDN.

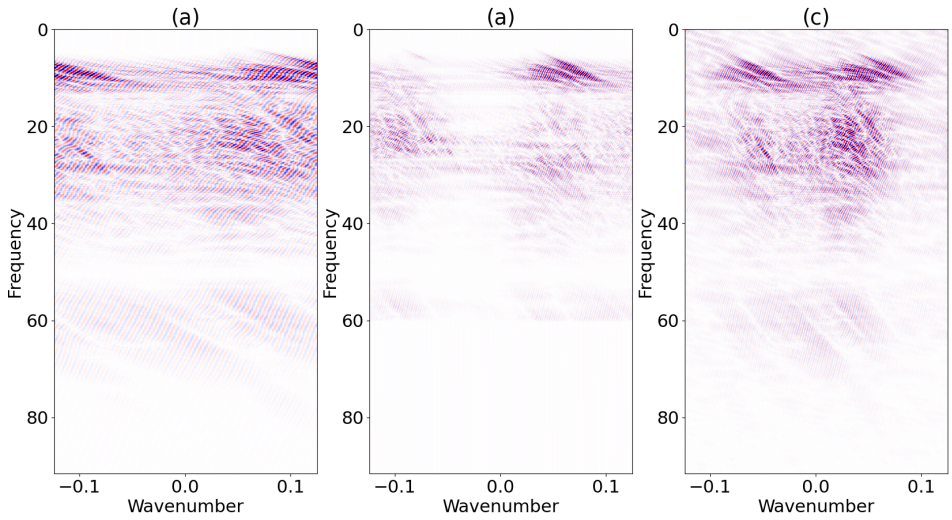

FIG. 16. F-k panel of the real shot gather 2. (a) F-K panel of the Original shot gather. (b) F-K panel of the interpolated shot gather via FX interpolation. (c) F-K panel of the interpolated shot gather via RDN.

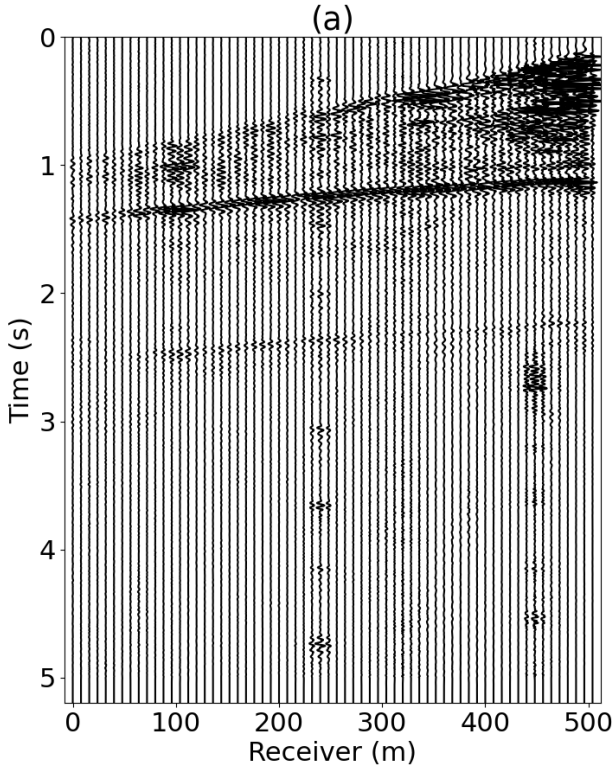

FIG. 17. Final result of real test 2 after interpolation and ground roll attenuation

CONCLUSIONS

We used a convolutional neural network-based framework called residual dense network (RDN) to interpolate the seismic data with strong ground noise. Unlike the conventional seismic interpolation methods based on the Fourier transform, spatial aliasing doesn't affect the proposed method. Examples prove that the Rdnet can reconstruct the reflections successfully, even if the amplitude of the reflections is much smaller than the ground roll. The interpolated result can be used for further processing and ground roll attenuation. The test results of the synthetic data example show a simple f-k filter can successfully remove the ground roll of the interpolated shot gather. However, conventional and machine learning methods do not work well with the actual ground data example, which needs further improvement.

ACKNOWLEDGMENTS

We thank the sponsors of CREWES for their continued support. This work was funded by CREWES industrial sponsors and NSERC (Natural Science and Engineering Research Council of Canada) through the grant CRDPJ 543578-19.

REFERENCES

Abadi, M., Barham, P., Chen, J., Chen, Z., Davis, A., Dean, J., Devin, M., Ghemawat, S., Irving, G., Isard, M. et al., 2016, Tensorflow: a system for large-scale machine learning., *in* Osdi, vol. 16, Savannah, GA, USA, 265–283.

Abma, R., and Kabir, N., 2006, 3d interpolation of irregular data with a pocs algorithm: Geophysics, **71**, No. 6, E91–E97.

Askari, R., and Siahkoohi, H. R., 2008, Ground roll attenuation using the s and x-f-k transforms: Geophysical Prospecting, **56**, No. 1, 105–114.

Beresford-Smith, G., and Rango, R., 1989, Suppression of ground roll by windowing in two domains: First Break, **7**, No. 2.

Deighan, A. J., and Watts, D. R., 1997, Ground-roll suppression using the wavelet transform: Geophysics, **62**, No. 6, 1896–1903.

Fang, W., Fu, L., Zhang, M., and Li, Z., 2021, Seismic data interpolation based on u-net with texture loss: Geophysics, **86**, No. 1, V41–V54.

Gao, J., Sacchi, M. D., and Chen, X., 2013, A fast reduced-rank interpolation method for prestack seismic volumes that depend on four spatial dimensions: Geophysics, **78**, No. 1, V21–V30.

Gao, J., Stanton, A., and Sacchi, M. D., 2015, Parallel matrix factorization algorithm and its application to 5d seismic reconstruction and denoising: Geophysics, **80**, No. 6, V173–V187.

Henley, D. C., 2003, Coherent noise attenuation in the radial trace domain: Geophysics, **68**, No. 4, 1408–1416.

Jia, Y., Yu, S., Liu, L., and Ma, J., 2016, A fast rank-reduction algorithm for three-dimensional seismic data interpolation: Journal of Applied Geophysics, **132**, 137–145.

Jiao, S., Chen, Y., Bai, M., Yang, W., Wang, E., and Gan, S., 2015, Ground roll attenuation using non-stationary matching filtering: Journal of Geophysics and Engineering, **12**, No. 6, 922–933.

Kaur, H., Pham, N., and Fomel, S., 2019, Seismic data interpolation using cyclegan, *in* SEG technical program expanded abstracts 2019, Society of Exploration Geophysicists, 2202–2206.

Kingma, D. P., and Ba, J., 2014, Adam: A method for stochastic optimization: arXiv preprint arXiv:1412.6980.

Li, H., Yang, W., and Yong, X., 2018, Deep learning for ground-roll noise attenuation, *in* SEG Technical Program Expanded Abstracts 2018, Society of Exploration Geophysicists, 1981–1985.

Liu, B., and Sacchi, M. D., 2004, Minimum weighted norm interpolation of seismic records: Geophysics, **69**, No. 6, 1560–1568.

Morse, P. F., and Hildebrandt, G. F., 1989, Ground-roll suppression by the stackarray: Geophysics, **54**, No. 3, 290–301.

Naghizadeh, M., and Sacchi, M. D., 2007, Multistep autoregressive reconstruction of seismic records: Geophysics, **72**, No. 6, V111–V118.

Pham, N., and Li, W., 2022, Physics-constrained deep learning for ground roll attenuation: Geophysics, **87**, No. 1, V15–V27.

Porsani, M. J., Silva, M. G., Melo, P. E., and Ursin, B., 2010, Svd filtering applied to ground-roll attenuation: Journal of Geophysics and Engineering, **7**, No. 3, 284–289.

Saatcilar, R., and Canitez, N., 1988, A method of ground-roll elimination: Geophysics, **53**, No. 7, 894–902.

Spitz, S., 1991, Seismic trace interpolation in the fx domain: Geophysics, **56**, No. 6, 785–794.

Trad, D., 2009, Five-dimensional interpolation: Recovering from acquisition constraints: Geophysics, **74**, No. 6, V123–V132.

Trad, D. O., Ulrych, T. J., and Sacchi, M. D., 2002, Accurate interpolation with high-resolution time-variant radon transforms: Geophysics, **67**, No. 2, 644–656.

Treitel, S., Shanks, J. L., and Frasier, C. W., 1967, Some aspects of fan filtering: Geophysics, **32**, No. 5, 789–800.

Trickett, S., Burroughs, L., Milton, A., Walton, L., and Dack, R., 2010, Rank-reduction-based trace interpolation, *in* 2010 SEG Annual Meeting, OnePetro.

Wang, B., Zhang, N., Lu, W., and Wang, J., 2019, Deep-learning-based seismic data interpolation: A preliminary result: Geophysics, **84**, No. 1, V11–V20.

Wang, W., Gao, J., Chen, W., and Xu, J., 2012, Data adaptive ground-roll attenuation via sparsity promotion: Journal of Applied Geophysics, **83**, 19–28.

Wang, Y., Wang, B., Tu, N., and Geng, J., 2020, Seismic trace interpolation for irregularly spatial sampled data using convolutional autoencodercae-based seismic trace interpolation: Geophysics, **85**, No. 2, V119–V130.

Yuan, Y., Si, X., and Zheng, Y., 2020, Ground-roll attenuation using generative adversarial networksground-roll attenuation using gans: Geophysics, **85**, No. 4, WA255–WA267.

Zhang, H., Ibrahim, A., Trad, D., and Innanen, K., 2019, Seismic trace interpolation using residual dense network.

Zhang, Y., Tian, Y., Kong, Y., Zhong, B., and Fu, Y., 2018, Residual dense network for image super-resolution, *in* Proceedings of the IEEE conference on computer vision and pattern recognition, 2472–2481.